

A Method of Predicting Unsteady Turbulent Flows and Its Application to Diffusers with Unsteady Inlet Conditions

A.A. Lyrio* and J.H. Ferziger†
Stanford University, Stanford, California

An integral method for computing the main characteristics of unsteady, incompressible, turbulent flows is developed. The method is applied to unsteady boundary layers with a prescribed freestream velocity and to diffusers with unsteady inlet conditions. For prescribed pressure gradient flows, the method gives as good results and is more than an order of magnitude faster than finite difference methods. For diffuser flows, no other methods have been found in the literature.

I. Introduction

UNSTEADY turbulent flows occur in a number of practical situations in fluids engineering. Turbulent detachment and reattachment are always somewhat unsteady, and oscillating turbulent flows occur in many systems. Examples are the boundary layer on a stationary vane downstream of a compressor, the flow over rotating turbine blades, and the diffuser downstream of a compressor in a gas turbine. Diffusers operating in the transitory stall regime have large-amplitude oscillations. The unsteady turbulent flow over a helicopter rotor blade is another important example. McCroskey¹ observes that the aerodynamic forces associated with unsteady separation can be stochastic or highly organized and periodic. Understanding these forces is fundamental to aerodynamic design.

Unsteady turbulent flow measurements are very difficult. Consequently, few results are given in the literature. Karlsson² reported experimental results for a turbulent boundary layer on a flat plate subjected to an oscillating freestream. His main conclusion was that nonlinear effects, even at the largest fluctuation amplitudes, were negligible. Miller³ reported results for heat transfer in an oscillating turbulent boundary layer similar to Karlsson's. With respect to the fluid dynamics, Miller confirmed Karlsson's conclusions. More recently, experiments involving flat-plate turbulent boundary layers subject to an oscillating stream have been done by the ONERA group led by Cousteix^{4,5} and also by Parikh et al.⁶

Unsteady, turbulent, fully developed channel flow measurements have been reported by Hussain and Reynolds⁷ and Acharya and Reynolds.⁸ McCroskey et al.⁹ reported a flow visualization experiment on the dynamic stall on oscillating airfoils. Schachenmann and Rockwell¹⁰ and Tomsho and Brown¹¹ performed experiments with low-speed air flow on oscillating turbulent boundary layers in conical diffusers, while Sajben and Kroutil¹²⁻¹⁴ have done experiments on unsteady transonic flows in two-dimensional diffusers.

On the computational side, the prediction of unsteady turbulent flows is currently undergoing active development. Most work has concentrated on laminar flows, but methods for unsteady turbulent flow have been based on steady-flow turbulence models. Good results have been obtained. This is not surprising, since Parikh et al. show that quasisteady

turbulence models are adequate for turbulent flat-plate flows in oscillating adverse pressure gradients.

McDonald and Shamroth¹⁵ used Cole's velocity profile, together with the momentum integral, energy integral, and continuity equations, to build an integral method able to compute unsteady compressible turbulent boundary layers. Kuhn and Nielsen¹⁶ used Coles' velocity profile and the moment of momentum integral equations, together with a quasisteady Clauser eddy-viscosity model to produce a linearized theory able to compute high frequency, unsteady, flat-plate flows. Telionis and Tsahalis¹⁷ integrated the time-dependent turbulent boundary-layer equations numerically, using a finite difference scheme, and were able to reproduce some high-frequency results and to approach detachment. McCroskey and Philippe¹⁸ computed flows on an oscillating airfoil and were able to reproduce some of the phase lead data of Karlsson's flat-plate flow. Singleton and Nash¹⁹ developed a finite difference method and computed the magnitude and phase shift of the displacement thickness and wall shear for two frequencies and amplitudes of an unsteady turbulent boundary layer. Recently, Cousteix and Houdeville^{4,5} have developed an integral method to predict the unsteady behavior of turbulent boundary layers.

The proceedings of the IUTAM Symposium on Unsteady Turbulent Shear Flows (Michel et al.²⁰) appeared while this paper was in review. This volume contains several papers of direct relevance to the current work; we shall be able to mention them only briefly here. Carr²¹ reviewed the experiment data in much more detail than we have been able to do here. Kobashi and Hayakawa²² presented data that complement the data we have used and which could have been used as targets for the present calculations. Parikh et al.²³ presented some further data; these were available to the current authors prior to their publication. Finally, Ramaprian and Tu²⁴ present data for a high-frequency oscillating tube flow that show variations from the equilibrium relationships used in many calculational schemes. However, it is not clear whether these contradict the current results, as we shall display good agreement with the high-frequency data.

The present paper develops a time-dependent integral method able to predict unsteady boundary layers in zero and adverse pressure gradients. Extensive comparison with the experimental data is made and good agreement is found. It also compares favorably with other time-dependent calculations. The method is extended to the computation of conical diffusers with unsteady inlet conditions; comparison to the sparse experimental data is made, again showing good agreement.

II. Integral Method for Unsteady Boundary Layers

The 1968 AFOSR-IFP-Stanford Conference²⁵ assembled the best integral methods for boundary layers available up to that time; since then others have been developed. Kuhn and

Presented as Paper 82-0349 at the AIAA 20th Aerospace Sciences Meeting, Orlando, Fla., Jan. 11-13, 1982; submitted Feb. 16, 1982; revision received June 21, 1982. Copyright © American Institute of Aeronautics and Astronautics, Inc., 1983. All rights reserved.

*Research Assistant, Thermosciences Division, Department of Mechanical Engineering; present address: Federal University of E. Santo, Vitoria, Brazil.

†Professor of Mechanical Engineering, Thermosciences Division, Department of Mechanical Engineering. Member AIAA.

Nielsen¹⁶ used an integral method to compute separating flows. Ghose and Kline²⁶ used a lag-entrainment method to compute diffusers in the early transitory stall regime. Lyrio et al.²⁷ extended their method to the computation of planar and conical diffusers operating in the unstalled, transitory stall, and fully developed stall regimes. Bardina et al.²⁸ extended this method to annular diffusers, and Childs et al.²⁹ extended it to compressible diffuser flows. For unsteady flows, integral methods have also been applied successfully. McDonald and Shamroth¹⁵ were the first to apply them to unsteady boundary layers. Kuhn and Nielsen¹⁶ and Cousteix⁵ also developed methods for prescribed pressure gradient, unsteady boundary-layer flows.

All integral methods use the momentum integral equation, a skin-friction correlation, a velocity profile assumption, and an auxiliary equation to close the system of equations. There is a variety of methods using different auxiliary equations. The entrainment method appears to work better than other methods for a variety of boundary-layer flows, and we shall adopt this choice.

A. Velocity Profile Family

The experiments of Houdeville and Cousteix⁴ show that imposed sinusoidal fluctuations do not alter the mean velocity profile from that of a steady turbulent flow. Figure 1 compares their phase-averaged data with Coles³⁰ "wall-wake law." Good agreement exists for every phase of the oscillations, even close to separation. Consequently, the wall-wake law may be assumed accurate for oscillating boundary layers. The use of Coles' profile leads to a shape-factor relation presented in Bardina et al.²⁸

$$h = 1.5\Lambda + 0.179V_T + 0.321V_T^2/\Lambda \quad (1)$$

where

$$h = \frac{H-1}{H} \quad \Lambda = \frac{\delta^*}{\delta} \quad V_T = \frac{1}{K} \sqrt{\frac{|\tau_w|}{\rho u_\infty^2}} \operatorname{sgn}(\tau_w)$$

and $K = 0.41$ is the von Kármán constant.

For the skin friction, a new correlation of Lyrio et al.²⁷ is used:

$$C_f/2 = .0325 |1 - 2\Lambda|^{1.77} (\Lambda/Re^*)^{0.115} \operatorname{sgn}(1 - 2\Lambda) \quad (2)$$

This correlation is explicit in terms of the skin friction and contains the criterion for separation implied by the Coles velocity profile.

The Cousteix⁵ experiments show that the turbulence structure is not altered by the fluctuations. This conclusion is verified by Parikh et al.⁶ The recent data of Ramaprian and Tu²⁴ indicate a possible problem at high frequencies, but the amplitudes are generally small at high frequencies so this may

not be a problem. Consequently, we shall use a quasisteady model for the turbulence at all frequencies.

B. Momentum Integral and Entrainment Equations

The unsteady momentum integral equation is obtained by phase-averaging the Navier-Stokes equations to produce equations for the phase-averaged velocity. When these equations are integrated across the boundary layer and combined in the usual way, we obtain an equation for the phase-averaged integral parameters:

$$\frac{\partial \theta}{\partial x} + (2+H) \frac{\theta}{u_\infty} \frac{\partial u_\infty}{\partial x} + \frac{1}{u_\infty^2} \frac{\partial}{\partial t} (\delta^* u_\infty) = \frac{C_f}{2} \quad (3)$$

where θ is the momentum thickness, δ^* the displacement thickness, and H the shape factor.

The rate of entrainment is defined in the same way as in the steady-state case:

$$E = \frac{1}{u_\infty} \frac{\partial}{\partial x} [u_\infty (\delta - \delta^*)] \quad (4)$$

In the present method, the quasisteady method developed by Lyrio et al.²⁷ is used. The method uses the lag equation

$$\frac{\partial E}{\partial x} = \frac{.025\Lambda}{\delta^*} (E' - E) \quad (5)$$

where the "equilibrium" entrainment E' is given by the correlation

$$E' = 4.24Ke[\Lambda/(1-\Lambda)]^{0.916} \quad (6a)$$

and

$$Ke = 0.013 + 0.0038e^{-\beta/15} \quad (6b)$$

$$\beta = \frac{\delta^*}{\tau_w} \frac{\partial p}{\partial x} \quad (6c)$$

For flows with adverse pressure gradients, the following simplified entrainment correlation,

$$E' = 0.0083(1-\Lambda)^{-2.5} \quad (7)$$

works quite well and does not require a lag. It is preferred for diffuser calculations owing to its ease of use and efficiency.

This completes the description of our method for boundary layers. As can be seen, all of the components of the steady-state method have been used without modification. The only change is the allowance for unsteadiness in the momentum integral equation. As we shall see below, this method works quite well.

III. Unsteady Boundary Layer with Prescribed Freestream Velocity

A. Method

The system of equations formed by the unsteady momentum integral equation (3), the entrainment correlation (5), and the Coles velocity profile is converted to the variables $\Lambda = \delta^*/\delta$ and $h = (H-1)/H$. The resulting equations are

$$(1+h+C_2) \frac{\partial \delta^*}{\partial x} - \delta^* C_1 \frac{\partial \Lambda}{\partial x} = \frac{C_f}{2} - (3-2h+C_2) \frac{\delta^*}{u_\infty} \frac{\partial u_\infty}{\partial x} - \frac{1}{u_\infty} \frac{\partial \delta^*}{\partial t} - \frac{\delta^*}{u_\infty^2} \frac{\partial u_\infty}{\partial t} \quad (8)$$

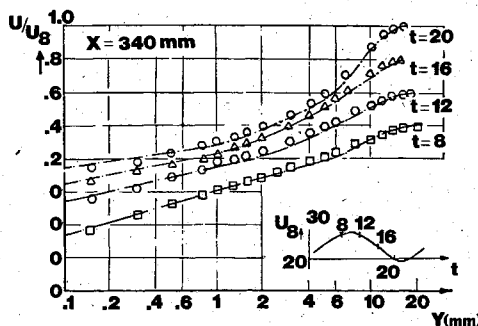


Fig. 1 Comparison of the Houdeville-Cousteix data for an unsteady adverse pressure gradient boundary layer with the Coles wall-wake law.

$$\frac{\partial \delta^*}{\partial x} - \frac{\delta^*}{\Lambda(1-\Lambda)} \frac{\partial \Lambda}{\partial x} = \frac{\Lambda}{1-\Lambda} E \quad (9)$$

where

$$C_2 = 0.115 V_T \left(0.179 + 0.321 \frac{V_T}{\Lambda} \right)$$

$$C_I = 1.5 - 0.321 \left(\frac{V_T}{\Lambda} \right)^2 + \frac{0.115 - 2\Lambda}{\Lambda}$$

$$\times 0.179 + 0.642 \frac{V_T}{\Lambda} (0.3 + 0.4\Lambda) Re^*{}^{-0.115}$$

$\partial u_\infty / \partial x$ and $\partial u_\infty / \partial t$ are given and the skin-friction coefficient is evaluated from Eq. (2).

Since this system of equations is hyperbolic, either of two approaches can be used. The first one is marches in x at each t level. When the end of the plate ($x=L$) is reached, the time is advanced. The equations are integrated in x by a standard ordinary differential equation solution method.

The second approach is based on knowing the conditions for all times at the upstream position and solving for the velocities at all times at the next station. This approach turned out to be more efficient and all the results given below were obtained using it.

B. Results for Zero Pressure Gradient

In this section, we consider oscillating flows with $\partial u_\infty / \partial x = 0$. Initial data are given at $x=0$. In order not to have to deal with the laminar and transition regimes, we used the boundary conditions given by Singleton and Nash.¹⁹ They defined the boundary-layer thickness at $x=0$ as

$$\frac{\delta_0(t)}{L} = a_1 \left(\frac{u_\infty(t)}{u_\infty} \right)^{-0.2}$$

This condition corresponds to the assumption that a steady

flat-plate boundary layer has developed upstream of $x=0$ at the instantaneous velocity $u_\infty(t)$. Similarly, we have

$$\frac{\delta_0^*(t)}{L} = a_2 \left(\frac{u_\infty(t)}{u_\infty} \right)^{-0.2}$$

Consequently, the boundary-layer blockage fraction Λ is constant at the initial station

$$\Lambda_0 = \frac{\delta_0^*(t)}{\delta_0(t)} = \frac{a_2}{a_1}$$

We shall compare our results with the data of Karlsson² and Houdeville and Cousteix⁴ and with the calculations of McCroskey and Philippe,¹⁸ Singleton and Nash,¹⁹ Kuhn and Nielsen,¹⁶ and Cousteix.⁵

Figure 2 presents a comparison between the experimental data and computational results for the displacement thickness phase-angle variation with frequency. The phase angle of δ^* relative to the freestream velocity increases for small values of the reduced frequency, reaches a maximum value of approximately 50 deg at a reduced frequency of 1, and decreases again at higher frequencies, going asymptotically to zero.

McCroskey and Philippe¹⁸ computed the displacement thickness amplitude and phase angle from Karlsson's data; the uncertainties shown in Fig. 2 were estimated by them. Our computation follows the trends of the data well and also compares well with the finite difference computational results. In the reduced frequency range 2-5, none of the methods follows Karlsson's data accurately. The Singleton-Nash results show lag behavior for reduced frequencies above 4, and do not regain the lead behavior at higher frequencies. At reduced frequencies above 5, the Cousteix computation shows oscillatory behavior. All previous computational results stop at reduced frequencies of the order of 16. This is mainly a consequence of the belief that the quasisteady turbulence models do not hold for frequencies of the order of the "burst" frequency ($\delta/u_0 \approx 0.1$, where f is in hertz). However, the experiments of Parikh et al.⁶ show that, as the frequency increases, the turbulent shear stress distribution becomes frozen at the steady-state distribution. Ramaprian and Tu's²⁴ recent data for tube flow are in disagreement with this observation; but, assuming it correct, we ran our code for reduced frequencies up to $\omega x/u_0 = 100$ without any problem. The phase-angle results tend asymptotically towards zero. This asymptotic behavior is also indicated by the data of Karlsson² and of Houdeville and Cousteix.⁴ The McCroskey and Cousteix results as well as our results indicate a weak Reynolds number dependence of the displacement thickness phase angle at reduced frequencies $\omega x/u_0 < 2$. For reduced frequencies above 2, all computational results show no dependence on the Reynolds number at all. They also indicate a large phase lead for reduced frequencies in the range $0.2 < \omega x/u_0 < 2$.

In Fig. 3, we give the displacement thickness amplitude vs reduced frequency. Again, our prediction follows Karlsson's data. The Cousteix computational results follow the trend up to a reduced frequency of 2, after which they oscillate. The results of McCroskey and Philippe¹⁸ are below ours, but the trend is the same. The data as well as the computational results show the asymptotic trend towards unity.

Figures 4 and 5 present the wall-shear results. Unfortunately, there are no data available. Telonis and Tshalis¹⁷ computed skin-friction phase angles from Karlsson's data. However, these data are very uncertain. Therefore we present only the computed results for the wall shear.

The three sets of computational results presented in Fig. 4 agree very well. Our computation shows an asymptotic trend toward the value of 2 for the nondimensional amplitude of the wall-shear oscillations at high frequency. For the wall-shear phase angle (Fig. 5), our computation shows an asymptotic

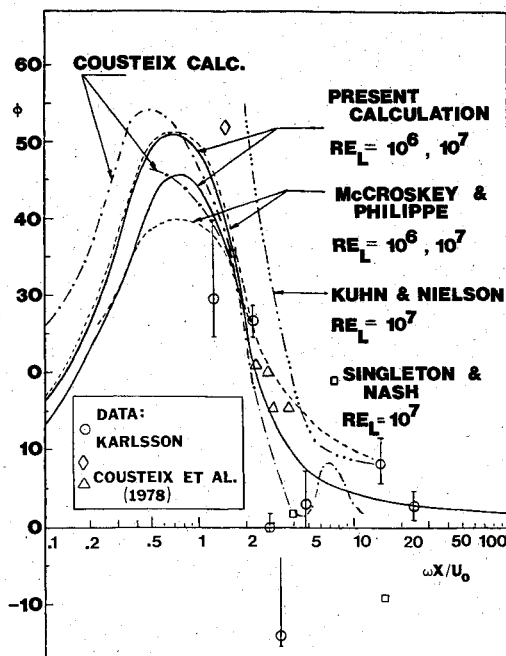


Fig. 2 Phase distribution of fluctuations on a flat plate in an oscillating stream. The velocity is $U_0(1 + 0.125 \sin \omega t)$; $\delta^* = \delta_0^* + 0.125 \delta_1^* \sin(\omega t + \pi + \phi)$.

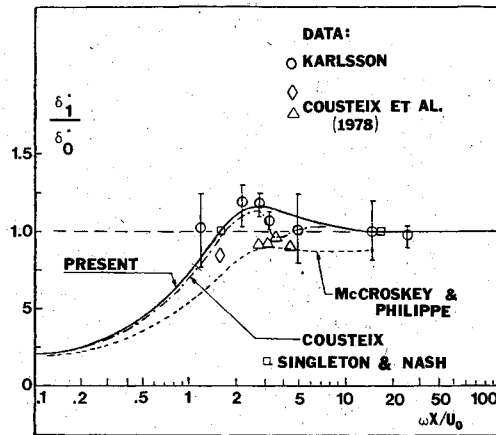


Fig. 3 Amplitude of the boundary-layer displacement thickness fluctuations for a flat plate in an oscillating stream. Conditions are as in Fig. 2.

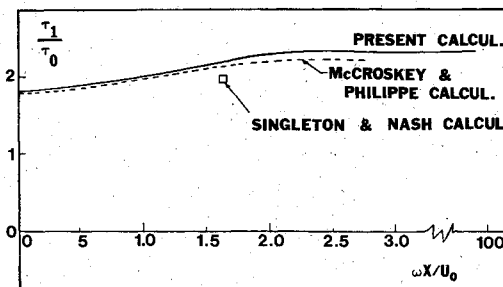


Fig. 4 Amplitude of the skin-friction fluctuations on a flat plate in an oscillating stream. Conditions as in Fig. 3; $\tau = \tau_0 + 0.125 \tau_1 \sin(\omega t + \phi)$.

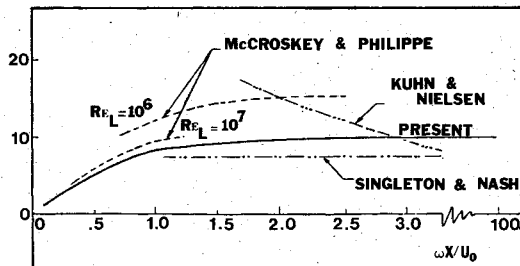


Fig. 5 Phase angle of skin-friction fluctuations on a flat plate in an oscillating stream. Conditions as in Fig. 4.

trend toward a lead of 10 deg. Singleton and Nash¹⁹ give a constant lead of 8 deg. The McCroskey-Philippe results compare well with our computational results for $Re_L = 10^7$. However, they found a Reynolds number dependence not shown by our computation. The results of Kuhn and Nielsen¹⁶ show a decrease in phase angle with increasing reduced frequency.

C. Results for Adverse Pressure Gradient

We ran two cases in which $\partial u_\infty / \partial x < 0$. The first case is the flow of Parikh et al.⁶ in which the starting conditions are those of an equilibrium flat-plate flow with constant freestream velocity. The second is the unsteady separating flow of Houdeville and Cousteix.⁴

In the Parikh et al. flow, the freestream oscillates around an average velocity that decreases linearly downstream. The amplitude of the fluctuations increases from zero at the starting point to a maximum of $0.5 u_{\infty,0}$ at the end of the plate. Under these conditions, the flow remains attached.

Figure 6 displays the velocity-amplitude distribution across the boundary layer. The overshoot in the velocity amplitude in the boundary layer for the quasisteady (zero frequency)

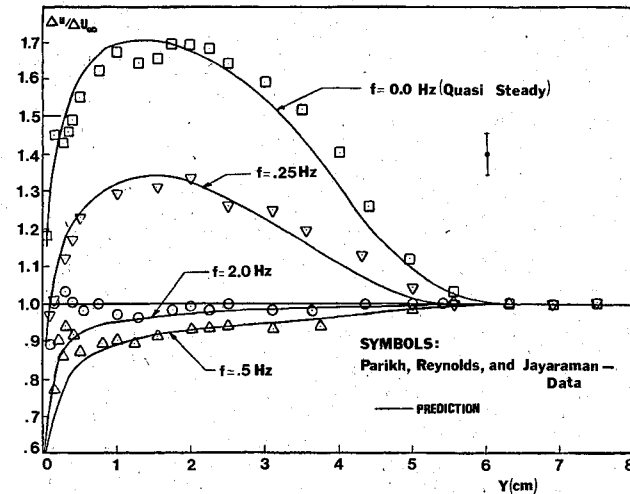


Fig. 6 Amplitude of velocity oscillations across an unsteady boundary layer.

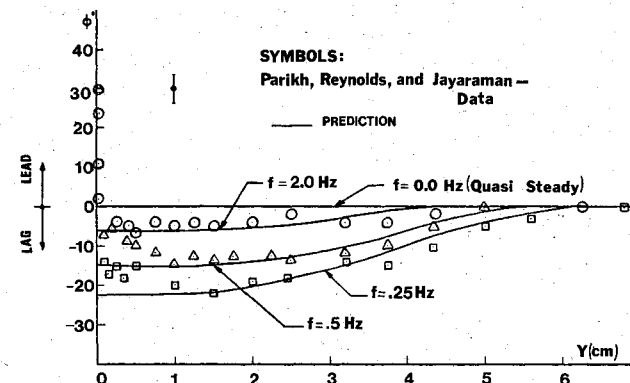


Fig. 7 Phase variation for the boundary layer of Fig. 6.

case is very well predicted. For 0.25 Hz, the prediction is excellent. The same is true at 0.5 and 2.0 Hz in the outer part of the boundary layer. However, close to the wall we underpredict the data by a few percent.

In Fig. 7 the phase variation of the velocity across the boundary layer is given. The results are excellent, except for the region close to the wall. At 2.0 Hz, the data show a lead close to the wall that our method is not able to reproduce. This is probably due to a Stokes layer whose thickness is comparable to the viscous sublayer thickness.

In Fig. 8 we compare our results to the Houdeville-Cousteix⁴ flat-plate data. Reverse flow appears during part of the cycle beyond $x = 450$ mm; we designate this point by the letter S. The frequency is much smaller than the "burst" frequency. The data in Fig. 8 are the time-averaged shape factor and displacement thickness. Our results are in good agreement with the data until the separation point and the location of separation is well predicted. After separation, we overpredict both δ_0^* and H_0 . Possible explanations of the difference are 1) that the data are uncertain, 2) that the Coles velocity profile or the entrainment correlation may not hold in the unsteady reverse-flow region, and 3) that one set of characteristics of the equations is reversed after separation and our solution method is mathematically invalid.

IV. Diffusers with Unsteady Inlet Conditions

A. Method

The diffuser method consists of the simultaneous solution of the boundary-layer equations given above with a one-dimensional core continuity equation. The inlet conditions are assumed known. As the flow is incompressible, the volume flow rate is the same at any section of the diffuser at each

instant of time and is a function of time only. Since the only data are for conical units, we shall consider that case.

The momentum integral equation for axisymmetric boundary layers is (see Lyrio et al.²⁷)

$$\frac{\partial \theta}{\partial x} + (2+H) \frac{\theta}{u_\infty} \frac{\partial u_\infty}{\partial x} + \frac{\theta}{R} \frac{dR}{dx} + \frac{1}{u_\infty^2} \frac{\partial}{\partial t} (u_\infty \delta^*) = \frac{C_f}{2} \quad (10)$$

and the entrainment equation is

$$\frac{1}{Ru_\infty} \frac{\partial}{\partial x} [Ru_\infty (\delta - \delta^*)] = E \quad (11)$$

The simpler entrainment correlation, Eq. (7), which does not need a lag equation was used here. For the velocity profile, the Coles "wall-wake law," Eq. (1), is again employed. For the skin friction, Eq. (2) is used.

The one-dimensional core continuity equation for conical geometries assumes the form

$$Q = \pi R_l^2 \left(1 - \frac{\delta_l^*(t)}{R_l} \right)^2 u_{\infty l}(t) \\ = \pi R^2(x) \left(1 - \frac{\delta^*(x,t)}{R(x)} \right)^2 u_\infty(x,t)$$

This equation is solved together with Eqs. (10) and (11) for the boundary layer. The system of equations is solved in the same way as the system for unsteady boundary layers. No numerical problems were encountered.

B. Results

In this section we present our computational results for a 6 deg conical diffuser, the only unsteady incompressible diffuser flow for which experimental data are available.

In Fig. 9, the core fluctuation amplitude normalized with respect to the inlet core velocity amplitude ($A=7\%$) is plotted. The computational results are compared to the data of Schachenmann and Rockwell¹⁰ for a reduced frequency $St = \omega L / u_i = 1$ (where $f = 5$ Hz). A similar comparison for reduced frequency $St = 7.33$ (where $f = 35$ Hz) and $A = 1.25\%$

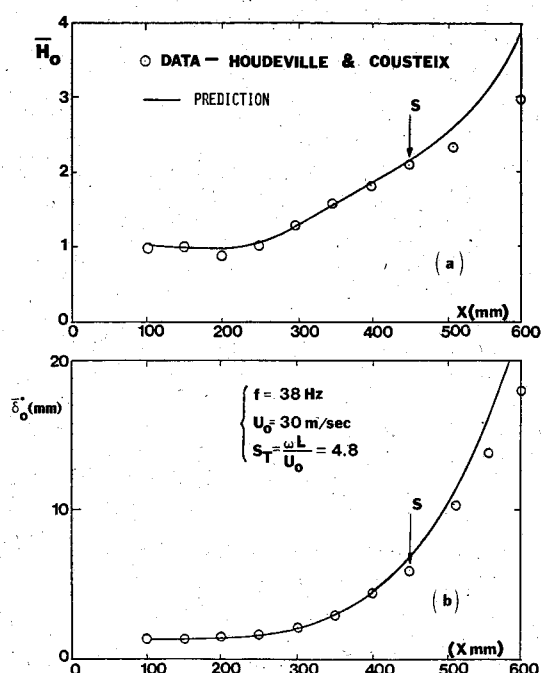


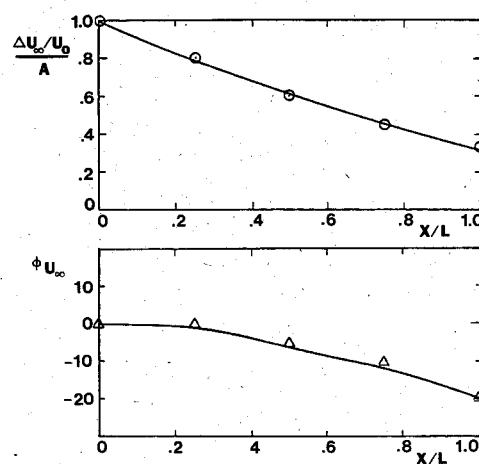
Fig. 8 The unsteady boundary layer of Houdeville and Cousteix. Upper figure gives the time-average shape factor; lower figure gives the time-averaged displacement thickness.

is given in Fig. 10. At the low frequency (Fig. 9), the velocity lags the inlet velocity all the way to the diffuser exit. However, for the higher frequency (Fig. 10) the computation indicates a lead between $x/L = 0.6$ and 0.8 . This is observed in the data of both Schachenmann and Rockwell¹⁰ and Tomsho and Brown.¹¹

In Fig. 11, we give the distribution of velocity amplitude across the boundary layer, the phase-angle distribution, and the time-averaged velocity. The dependence of the time-averaged velocity on frequency seems to be negligible; this is consistent with Parikh et al.⁶

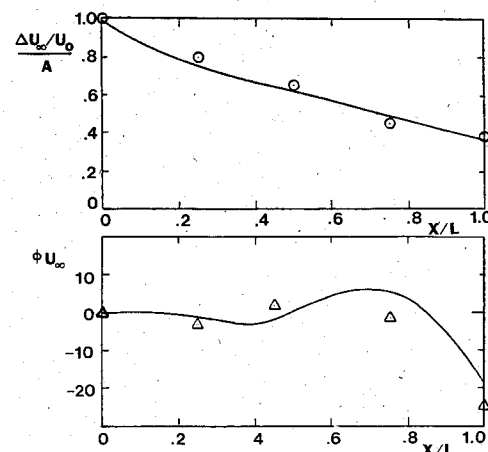
Figure 12 gives the boundary-layer velocity-amplitude distribution along the diffuser wall for $St = 1.0$ and $A = 7\%$. The agreement is excellent, except at the diffuser exit, where we underpredict the velocity amplitude in the outer region of the boundary layer. A possible explanation for the underprediction at the diffuser exit is that the conditions beyond the exit influence the velocity profile measurements at that station.

In Fig. 13, the phase-angle distribution across the boundary layer is presented for different positions along the diffuser



○ DATA: SCHACHENMANN & ROCKWELL
— COMPUTATIONAL RESULTS

Fig. 9 The velocity fluctuation amplitude (upper curve) and phase (lower curve) for the 6-deg unsteady conical diffuser of Schachenmann and Rockwell with 7% inlet fluctuation and $St = 1$.



○ DATA: SCHACHENMANN & ROCKWELL

— COMPUTATIONAL RESULTS

Fig. 10 The velocity fluctuation amplitude (upper curve) and phase (lower curve) for the 6-deg unsteady conical diffusers of Schachenmann and Rockwell with 1.25% inlet fluctuation and $St = 7.33$.

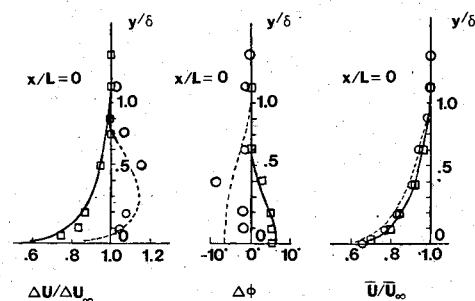
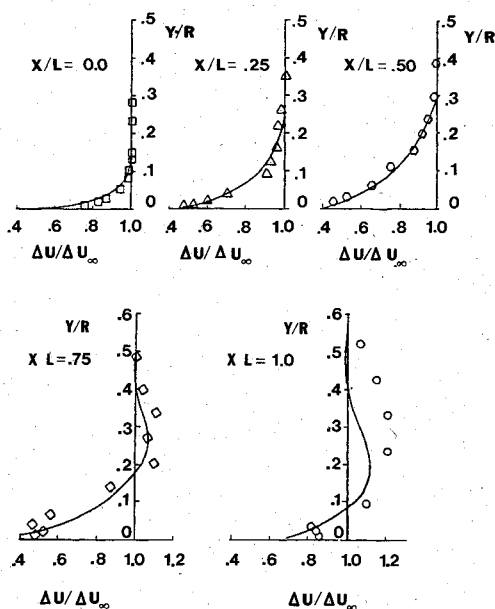
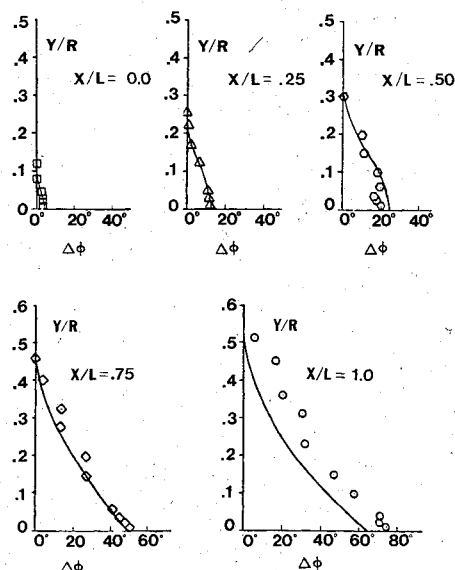


Fig. 11 Amplitude, phase-angle, and average velocity distributions across the boundary layer in the conical diffusers of Schachenmann and Rockwell. \square and — indicate the 7% amplitude, $St = 1$ case; \circ and - - - represent the 1.25% amplitude, $St = 7.33$ case.



6° CONICAL DIFFUSER

Fig. 12 Velocity-amplitude distribution at various positions along the diffuser wall for the Schachenmann and Rockwell 6-deg conical diffuser with 7% amplitude and $St = 1$.



6° CONICAL DIFFUSER

Fig. 13 Velocity phase-angle distribution along the diffuser wall for the Schachenmann and Rockwell 6-deg conical diffuser with 7% amplitude and $St = 1$.

wall for $A = 7\%$ and $St = 1.0$. Lead behavior is evident at all stations. The prediction follows the data very closely, except again at the diffuser exit. This may be due to the reason given above.

An important conclusion, which has been observed by all experimentalists in this area except Ramaprian and Tu,²⁴ is that the oscillating external flow does not affect the time-averaged boundary-layer profile. In the case of diffusers, so long as stall is not present, this implies that unsteady inlet flow does not alter the time-averaged diffuser performance.

V. Conclusions

An improved integral method for turbulent boundary layers has been developed. The method can handle detachment without difficulty and can do both the steady and unsteady cases.

Simultaneous solution of the boundary-layer equations and a one-dimensional continuity equation for the core flow gives a method for predicting diffuser flows with unsteady inlet conditions.

The results of the method show excellent or good agreement with the main features of all of the unsteady data available. This includes attached and detached boundary layers and unsteady diffusers.

The method is very simple and computationally very fast. The accuracy is comparable to that of the best finite difference methods available and is at least one order of magnitude faster.

The computations show that the mean flow parameters of boundary layers and diffusers are almost unaffected by oscillations. The experimental data available for these flows also lead to the same conclusions.

For the unsteady boundary layers, the method does not capture all of the characteristics close to the wall. We believe that this can be remedied in a simple way and will report on such an attempt later.

Acknowledgments

This work was supported by the U.S. Air Force Office of Scientific Research under Contract AF-F49620-79-C-0010. The authors would like to thank Dr. Juan Bardina, Professor S.J. Kline, Dr. R.E. Childs, and Roger Strawn for their important contributions to this work.

References

- McCroskey, W.J., "Some Current Research in Unsteady Fluid Dynamics—The 1976 Freeman Scholar Lecture," *Transactions of the ASME, Journal of Fluids Engineering*, Vol. 99, Series I, 1977, pp. 8-38.
- Karlsson, S.K.F., "An Unsteady Turbulent Boundary Layer," *Journal of Fluid Mechanics*, Vol. 5, Pt. 4, 1958.
- Miller, J.A., "Heat Transfer in the Oscillating Turbulent Boundary Layer," *Transactions of the ASME, Journal of Engineering for Power*, Oct. 1969.
- Houdeville, R. and Cousteix, J., "Premiers Resultats d'une Etude sur les Couches Limites Turbulentes en Ecoulement Pulse avec Gradient de Pression Moyen Favorable," ISE Colloque d'Aerodynamique, AAAF NT-79-05, Nov. 1978; see also NASA TN-75799 (English translation).
- Cousteix, J., "Couches Limites en Ecoulement Pulse," ONERA Rept. No. NT-1979-1, 1979.
- Parikh, P.G., Reynolds, W.C., and Jayaraman, R., "On the Behavior of an Unsteady Turbulent Boundary Layer," *Numerical and Physical Aspects of Aerodynamic Flows*, edited by T. Cebeci, Springer, 1982.
- Hussain, A.K.M.F. and Reynolds, W.C., "The Mechanics of an Organized Wave in Turbulent Shear Flow," *Journal of Fluid Mechanics*, Vol. 41, Pt. 2, 1970, pp. 241-258.
- Acharya, M. and Reynolds, W.C., "Measurements and Predictions of a Fully Developed Turbulent Channel Flow with Imposed Controlled Oscillations," Rept. No. TF-8, Thermosciences Division, Department of Mechanical Engineering, Stanford University, Stanford, Calif., May 1975.

⁹McCroskey, W.J., Carr, L.W., and McAlister, K.W., "Dynamic Stall Experiments on Oscillating Airfoils," *AIAA Journal*, Vol. 14, Jan. 1976.

¹⁰Schachenmann, A.A. and Rockwell, D.O., "Oscillating Turbulent Flow in a Conical Diffuser," *Transactions of the ASME, Journal of Fluids Engineering*, Dec. 1976.

¹¹Tomsho, M.E. and Brown, F.T., "The Oscillating Turbulent Boundary Layer in a Conical Diffuser," in *Nonsteady Fluid Dynamics*, edited by D.E. Crow, ASME, 1978.

¹²Sajben, M. and Kroutil, J.C., "Unsteady Transonic Diffuser Flows in a Two-Dimensional Diffuser," McDonnell-Douglas Research Laboratories, Rept. No. MDC Q0651, 1978.

¹³Sajben, M. and Kroutil, J.C., "Unsteady Transonic Flows in a Two-Dimensional Diffuser," McDonnell-Douglas Research Laboratories, Rept. No. AFOSR-TR-79-0990, 1979.

¹⁴Sajben, M. and Kroutil, J.C., "Effects of Approach Boundary-Layer Thickness on Oscillating, Transonic Diffuser Flows, Including a Shock," McDonnell-Douglas Research Laboratories, Rept. No. MDRL 80-2, 1980.

¹⁵McDonald, H. and Shamroth, S.J., "An Analysis and Application of the Time-Dependent Turbulent Boundary Layer Equations," *AIAA Journal*, Vol. 9, Aug. 1971, pp. 1553-1560.

¹⁶Kuhn, G.D. and Nielsen, J.N., "Studies of an Integral Method for Calculating Time-Dependent Turbulent Boundary Layers," TR NEAR-2-PU, Project SQUID, 1973; see also "Flow Separation," *AGARD Conference Proceedings No. 168*, Paper 26, May 1975.

¹⁷Telionis, D.P. and Tsahalis, D. Th., "Unsteady Turbulent Boundary Layers and Separation," *AIAA Journal*, Vol. 14, 1976, pp. 468-474.

¹⁸McCroskey, W.J. and Philippe, J.J., "Unsteady Viscous Flow on Oscillating Airfoils," *AIAA Journal*, Vol. 13, Jan. 1975, pp. 71-79.

¹⁹Singleton, R.E. and Nash, J.F., "Method for Calculating Unsteady Turbulent Boundary Layers in Two- and Three-Dimensional Flows," *AIAA Journal*, Vol. 12, May 1974, pp. 590-595.

²⁰Michel, R., Cousteix, J., and Houdeville, R., "Unsteady Turbulent Shear Flows," *Proceedings, IUTAM Symposium*, Toulouse, France, Springer, Berlin, 1981.

²¹Carr, L.W., "A Review of Unsteady Turbulent Boundary Layer Experiments," *Proceedings, IUTAM Symposium*, Toulouse, France, Springer, Berlin, 1981.

²²Kobashi, Y. and Hayakawa, M., "Structure of Turbulent Boundary Layer on an Oscillating Flat Plate," *Proceedings, IUTAM Symposium*, Toulouse, France, Springer, Berlin, 1981.

²³Parikh, P., Reynolds, W.C., Jayaraman, R., and Carr, L.W., "Dynamic Behavior of an Unsteady Turbulent Boundary Layer," *Proceedings, IUTAM Symposium*, Toulouse, France, Springer, Berlin, 1981.

²⁴Ramaprian, B.R. and Tu, S.W., "Periodic Turbulent Pipe Flow at 'High' Frequencies of Oscillation," *Proceedings, IUTAM Symposium*, Toulouse, France, Springer, Berlin, 1981.

²⁵Kline, S.J., Morkovin, G., Sovran, G., and Cockrell, D.J., "Computation of Turbulent Boundary Layers—1968 AFOSR-IFP-Stanford Conference," Thermosciences Div., Mech. Engrg. Dept., Stanford Univ., 1968.

²⁶Ghose, S. and Kline, S.J., "Prediction of Transitory Stall in Two-Dimensional Diffusers," Rept. No. MD-36, Thermosciences Division, Department of Mechanical Engineering, Stanford University, Stanford, Calif., Dec. 1976; see also *Transactions of the ASME, Journal of Fluids Engineering*, Series I, Vol. 100, Dec. 1978, p. 419.

²⁷Lyrio, A.A., Ferziger, and Kline, S.J., "An Integral Method for the Computation of Steady and Unsteady Turbulent Boundary Layer Flows, Including the Transitory Stall Regime in Diffusers," Rept. No. PD-23, Thermosciences Division, Department of Mechanical Engineering, Stanford University, Stanford, Calif., March 1981.

²⁸Bardina, J.G., Kline, S.J., and Ferziger, J.H., "A Prediction Method for Diffuser Flow at Low Mach Numbers, Including a New Correlation for Detachment and Reattachment," Rept. No. PD-22, Thermosciences Division, Department of Mechanical Engineering, Stanford University, Stanford, Calif., 1981.

²⁹Childs, R., Ferziger, J.H., and Kline, S.J., "A Prediction for Compressible Flow in Planar Diffusers," Rept. No. PD-24, Thermosciences Division, Department of Mechanical Engineering, Stanford University, Stanford, Calif., 1981.

³⁰Coles, D.E., "The Law of the Wake in Turbulent Boundary Layers," *Journal of Fluid Mechanics*, Vol. 1, 1956, pp. 191-226.

AIAA Meetings of Interest to Journal Readers*

Date	Meeting (Issue of <i>AIAA Bulletin</i> in which program will appear)	Location	Call for Papers†
1983			
April 11-13	AIAA 8th Aeroacoustics Conference (Feb)	Terrace Garden Inn Atlanta, Ga.	July/Aug. 82
May 2-4	24th AIAA/ASME/ASCE/AHS Structures, Structural Dynamics & Materials Conference (Mar.)	Sahara Hotel Lake Tahoe, Nev.	June 82
May 10-12	AIAA Annual Meeting and Technical Display	Long Beach Convention Center Long Beach, Calif.	
June 1-3	AIAA 18th Thermophysics Conference (Apr.)	The Queen Elizabeth Hotel, Montreal, Quebec, Canada	Sept. 82
June 27-29	AIAA/SAE/ASME 19th Joint Propulsion Conference and Technical Display (Apr.)	Westin Hotel Seattle, Wash.	Sept. 82
July 12-14	AIAA 16th Fluid and Plasma Dynamics Conference (May)	Radisson Ferncroft Hotel and Country Club, Danvers, Mass.	Oct. 82
July 13-15	AIAA 6th Computational Fluid Dynamics Conference (May)	Radisson Ferncroft Hotel and Country Club, Danvers, Mass.	Oct. 82
July 13-15	AIAA Applied Aerodynamics Conference (May)	Radisson Ferncroft Hotel and Country Club, Danvers, Mass.	Oct. 82

*For a complete listing of AIAA meetings, see the current issue of the *AIAA Bulletin*.

†Issue of *AIAA Bulletin* in which Call for Papers appeared.

‡Cosponsored by AIAA. For program information, write to: AIAA Meetings Department, 1290 Avenue of the Americas, New York, N.Y. 10104.